A complete identification of lithium sites in a model of $LiPO_3$ glass: effects of the local structure and energy landscape on ionic jump dynamics

Michael Vogel*
Department of Chemical Engineering and Department of Materials Science and Engineering, University of Michigan, 2300 Hayward, Ann Arbor, MI, 48109, USA†

(Dated: February 2, 2008)

We perform molecular dynamics simulations to study lithium dynamics in a model of $LiPO_3$ glass at temperatures below the glass transition. A straightforward analysis of the ionic trajectories shows that lithium diffusion results from jumps between sites that are basically unmodified on the time scale of the lithium ionic relaxation. This allows us a detailed identification and characterization of the sites. The results indicate that the number of lithium sites is only slightly bigger than the number of lithium ions so that the fraction of vacant sites is very limited at every instant. Mapping the ionic trajectories onto series of jumps between the sites provides direct access to lithium jump dynamics. For each site, we determine the mean residence time τ_s of an ion and the probability p_s^b that a jump from this site to another site is followed by a direct backjump. While a broad distribution $G(\lg \tau_s)$ shows that different sites feature very diverse lithium dynamics, high values of p_s^b give direct evidence for correlated back-and-forth jumps. A strong decrease of p_s^b with increasing τ_s indicates that the backjump probability depends on the dynamical state of an ion. Specifically, we find that correlated back-and-forth jumps are important at short times in the relaxation process, but not on the time scale of the lithium relaxation, where the hopping motion resembles a random walk. We further study how the local glass structure and the local energy landscape affect lithium jump dynamics. We observe substantial effects due to the energy landscape, which are difficult to capture within single-particle approaches. Our results rather imply that lithium migration is governed by the competition of the ions for a small fraction of vacant sites in a disordered energy landscape. Consistently, a statistical analysis shows that a vacancy mechanism dominates the repopulation of the lithium sites.

PACS numbers: 66.30.Dn

I. INTRODUCTION

The mechanism for fast ion transport in glasses has challenged the combined efforts of industrial and scientific research over the last decades.[1,2,3] It is now well established that the macroscopic charge transport results from hopping of mobile ions between localized states in the glassy matrix.[1,3] However, the mechanism of this hopping motion is complex and several coexisting models seek to rationalize the very rich phenomenology of ionic glasses. While several authors postulated that ionic migration is governed by the Coulomb interactions among the mobile ions,[4,5,6] others stressed the relevance of the disordered energy landscape provided by the glassy matrix,[7,8,9] and percolation approaches were applied for a quantitative description of ionic diffusion.[10,11,12] The combined effect of these interactions was also regarded as important.[13,14,15,16] In addition, it was argued that structural properties, e.g., microsegregation of the mobile ions, play a major role for ion dynamics.[16,17] Also, the relevance of substantial relaxation of the glass structure below the glass transition temperature T_g was emphasized.[18]

To decide between different models of ion transport in glasses, detailed information about the ionic motion is required. For example, it is interesting whether all ions make the same contribution to the macroscopic charge transport or whether a distribution of mobilities exists. Further, the relevance of correlated back-and-forth jumps needs to be quantified. Due to this effect, which is one of the cornerstones of various modelling approaches, the dc conductivity σ_{dc} can be much smaller than expected based on the ionic jump rates. These points are related to the question about the origin of the nonexponential ionic relaxation, observed in electrical and mechanical relaxation studies.[2,19,20,21,22] Such behavior can result from two fundamentally different scenarios.[23] In the heterogeneous scenario, all particles are random walkers, but a distribution of jump rates exists. In the homogeneous scenario, all particles obey the same relaxation function that is intrinsically nonexponential due to correlated back-and-forth jumps. Additionally, it is intriguing to study how ion dynamics depends on the local glass structure.

Measuring the frequency dependent electric conductivity $\sigma(\nu)$, an experimental study of ion dynamics is possible. While the frequency independent value at low frequencies, σ_{dc}, is an important material parameter, a strong dispersion at higher frequencies indicates the presence of correlated back-and-forth motions.[6,24,25,26,27] Multidimensional nuclear magnetic resonance (NMR) experiments provide direct access to ionic jump dynamics.[28,29,30,31,32] Applications on crystalline and glassy silver ion conductors showed that the nonexponential depopulation of the silver sites is due to a distribution of jump rates, i.e., dynamic heterogeneity, rather than to an intrinsic noneponentiality.[31,32] In other words, no evidence for back-and-forth jumps was found, at variance

with conclusions from electric conductivity studies.

In molecular dynamics (MD) simulations, the trajectories of all particles are known and, thus, unique microscopic insights are available. Applications on ionic glasses confirmed that the dynamics of the mobile ions can be decomposed into vibrations about sites and occasional jumps between them.[33,34,35,36,37,38,39,40,41,42,43,44] Most simulation studies of ionic jump dynamics focused on alkali silicate glasses. For lithium silicate glasses, it was demonstrated that both homogeneous and heterogeneous dynamics contribute to the nonexponentiality of ionic relaxation.[40,43] For sodium silicate glasses, no evidence for back-and-forth jumps was found, but there are dynamic heterogeneities.[45,46,47,48,49] Specifically, fast ion transport was observed along preferential pathways, where, however, the presence of these channels was not attributed to a microsegregation of the sodium ions, as proposed by other workers.[16,50]

Very recently, we performed MD simulations to study ion dynamics in an alkali phosphate glass.[44] Based on multitime correlation functions, we demonstrated that the nonexponential lithium relaxation in $LiPO_3$ glass results from both correlated back-and-forth jumps and a broad distribution of jump rates. A quantitative analysis showed that the relevance of the heterogenous contribution increases with decreasing T. In addition, we observed an exchange between fast and slow lithium ions that occurs on the timescale of the jumps themselves. Thus, the dynamic heterogeneities are short lived, indicating that sites featuring fast and slow lithium dynamics, respectively, are intimately mixed.

Heuer and coworkers[51] used a computational approach to demonstrate that determination of the lithium sites in lithium silicate glasses provides new insights into the mechanism for ionic diffusion. A complete identification of the sites from the ionic trajectories showed that the number of sites is only slightly bigger than the number of ions, implying that ion dynamics is most appropriately described in terms of mobile vacancies. For a detailed study of the jump diffusion mechanism, the alkali trajectories were mapped onto sequences of jumps between the sites.[51] An analysis of these sequences revealed that the tendency for back-and-forth jumps depends on the dynamical state of an ion. Specifically, the back-jump probabilities are high when the lithium ions have escaped from sites characterized by comparatively short residence times.

In the present MD simulation approach, we investigate lithium jump dynamics in $LiPO_3$ glass via identification of the lithium sites. In particular, we study the effects of the local glass structure and the local energy landscape on the lithium hopping motion. To unravel the origin of the pronounced dynamic heterogeneities observed for this model glass in our previous work,[44] we analyze which factors determine the residence time at a site. Such analysis is also performed for the correlated back-and-forth jumps so that the present study may shed a light on the question why previous experimental and computational studies came to different conclusions about the relevance of this phenomenon. Furthermore, we use a statistical approach to ascertain the dominant mechanism for the repopulation of the lithium sites. All analyses are carried out in a temperature range, where the phosphate glass matrix, apart from local fluctuations, is rigid on the 20 ns-time scale of our simulation, while the lithium ionic subsystem can still be equilibrated.

II. MODEL AND SIMULATION DETAILS

The interactions of the ions in the studied model of $LiPO_3$ glass are described by the potential

$$\Phi_{\alpha\beta}(r) = \frac{q_\alpha q_\beta\, e^2}{r} + A_{\alpha\beta}\, \exp\left(-r/\rho\right), \qquad (1)$$

where e is the elementary charge and r denotes the distance between two ions of type α and β, respectively ($\alpha, \beta \in \{\mathrm{Li}, \mathrm{O}, \mathrm{P}\}$). Karthikeyan et al.[52] adjusted the parameters of this potential to enable a realistic description of the structure of $LiPO_3$ glass. They showed that, though there may be some deviations in the intermediate range order,[53] the simulated glass consists of well defined phosphate tetrahedra that are connected by two of their corners to form long chains and/or rings,[52] in agreement with experimental findings.[54,55,56] In previous work,[44] we studied the dynamical behavior of this model using a slightly modified set of potential parameters. We found that the dynamics of the atomic species decouple with decreasing T. While the structural relaxation of the phosphate network freezes in at a computer glass transition temperature $T_g \approx 1000\,\mathrm{K}$, fast lithium ionic diffusion takes place at $T < T_g$. Thus, it is possible to equilibrate the lithium ionic subsystem at $T < T_g$ and to study ionic migration in a glassy matrix. Detailed analysis of the lithium dynamics showed that the dynamical behavior of the model resembles that of $LiPO_3$ glass.[44]

In the present work, we identify the lithium sites in this model of $LiPO_3$ glass. For this purpose, we extend the temperature range of our previous study[44] to lower T, where lithium dynamics is well described as hopping motion. We perform MD simulations in the NVE ensemble with $\rho = 2.15\,\mathrm{g/cm^3}$ and $N = 800$ so that the number of lithium ions $N_{\mathrm{Li}} = 160$. Such moderate system size allows us to equilibrate the lithium ionic subsystem at sufficiently low T, while major finite size effects are absent.[44] The density is chosen based on the experimental value at room temperature, $\rho = 2.25\,\mathrm{g/cm^3}$,[57] together with the thermal expansion coefficient of $LiPO_3$ glass.[58] The equations of motion are integrated using the velocity Verlet algorithm with a time step of 2 fs, periodic boundary conditions are applied and the Coulombic forces are calculated via Ewald summation.[44]

Our simulations start from a configuration that was obtained previously[44] by equilibrating the phosphate network slightly above T_g, quenching into the glass and equilibrating the lithium ionic subsystem at $T = 590\,\mathrm{K}$. To set

the target temperatures of the present study, $T = 390\,\mathrm{K}$, $T = 450\,\mathrm{K}$ and $T = 520\,\mathrm{K}$, we first propagate this configuration while periodically rescaling the velocities. Afterwards, equilibration periods of lengths $t_{eq} = 30-40\,\mathrm{ns}$ without velocity scaling are applied at each T. Finally, we perform production runs of length $t_{sim} = 20\mathrm{ns}$. For $T = 520\,\mathrm{K}$, all lithium ions exit their sites during the equilibration period t_{eq}, indicating that the lithium ionic subsystem is well equilibrated. For the lower T, this condition cannot be met. However, apart from fluctuations, the temperature is constant after t_{eq} and, hence, the population of the lithium sites has reached its equilibrium distribution. Such behavior becomes reasonable based on our result that the number of lithium sites is very limited, see below, so that sites with long residence times and low energies are occupied in any case and equilibration only requires the repopulation of sites with short residence times and high energies, between which numerous exchange processes take place during the applied equilibration periods.

To further check the equilibration of the lithium ionic subsystem, we calculate the incoherent intermediate scattering functions of the lithium ions, see Fig. 3, and determine the mean time constants of the decays, as was done previously.[44] Comparison of previous and present results shows that all data at $T < T_g$ are well described by an Arrhenius law with activation energy $E_a = 0.47\,\mathrm{eV}$. Fitting data for both $T > T_g$ and $T < T_g$, we found a bigger value $E_a = 0.62\,\mathrm{eV}$ in our previous study.[44] Detailed inspection, however, shows that this difference can be traced back to a change in the temperature dependence at $T \approx T_g \approx 1000\,\mathrm{K}$. Based on these findings, we conclude that the lithium ionic subsystem is equilibrated at all T studied here.

III. IDENTIFICATION OF LITHIUM SITES

Following Heuer and coworkers,[51] a straightforward algorithm is applied to identify the lithium sites based on the MD trajectories. In detail, we first divide the simulation box into cubic cells of size $(0.3\,\mathrm{Å})^3$, which is sufficiently small so as to resolve the shape of the sites. For each T, we then determine the number of times, m, the cells are visited by a lithium ion during $t_{sim} = 20\mathrm{ns}$, where configurations separated by a time increment $\Delta t = 0.2\,\mathrm{ps}$ are analyzed. The visited cells thus constitute the lithium sites and the pathways between them. To eliminate the pathways, only cells with $m > m_0$ are considered in a following cluster analysis, where cells sharing a common face are grouped into one site. The value of m_0 is determined by the criterion that the number of distinct lithium sites be maximum. While lithium sites that are occupied less frequently are not detected for high values of m_0, different sites merge for small values of m_0 due to inclusion of the connecting pathways.

Having identified the lithium sites, the migration of the lithium ions can be mapped onto sequences of jumps between these sites. When an ion has left a site, it can either move to a new site or return to the old one. While we record the former event as a jump, we dismiss the latter and regard the residence at the particular site as not interrupted. In this way, we can exclude the effect of occasional large amplitude vibrations, which lead to exploration of volume outside the sites, but not to long-range transport. Thus, the residence time of a lithium ion at a site is defined as the interval between the time when the ion jumps into this site and the time when the ion exits this site in order to enter *another* site. Based on the residence times, we calculate both the mean residence time τ_s at a site and the mean number of lithium ions at a site, or, equivalently, the occupation number n_s. To determine τ_s, a sufficiently large number of jump processes has to be analyzed. This is possible for $T = 520\,\mathrm{K}$, whereas some sites are repopulated just a few times during t_{sim} at the lower T. To reduce the effect of the limited time window, we multiply the residence times at the beginning and at the end of the production run by a factor of two when calculating τ_s.

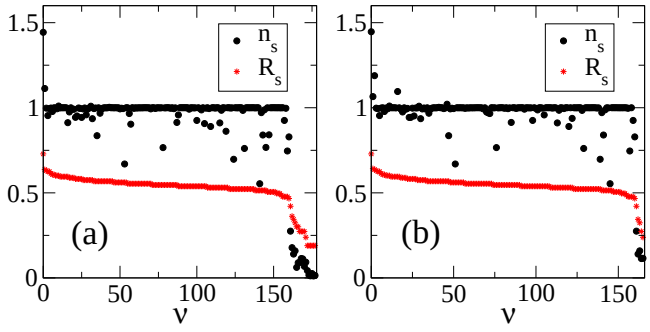

FIG. 1: Effective radius $R_s = (3V/4\pi)^{1/3}$ of the lithium sites and mean number n_s of lithium ions at a site. (a) Results for 178 sites obtained from a preliminary analysis at $T = 390\,\mathrm{K}$. (b) Results for the final set of 166 sites determined by eliminating satellite and transition sites, see text for details. In both panels, the sites are sorted according to their effective radius, which is plotted in units of Å, and ν denotes the site index.

Heuer and coworkers[51] observed that some small sites resulting from the described algorithm do not serve as independent sites, but they are satellites of larger sites or saddle-like states that are visited for a short period of time during the transitions between larger sites. Therefore, these small sites were excluded from their analysis. In view of these results, we determine the lithium sites in two steps. First, we identify the maximum number of sites at each T and study their nature in a preliminary analysis. Based on the findings, we then eliminate satellite and transition sites and perform the final analysis for the resulting set of sites, which turns out to be temperature independent.

The preliminary analysis yields between 176 and 193 lithium sites at the studied T. While 166 sites are present at all T (A sites), there is an additional temperature de-

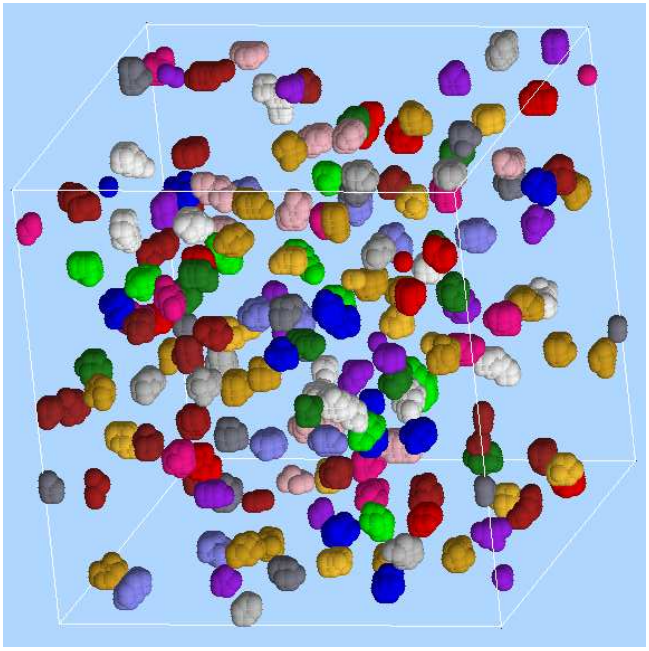

FIG. 2: Lithium sites in $LiPO_3$ glass. The sites were obtained by dividing the simulation box into small cubic cells and counting the number of times a particular cell is visited by a lithium ion in the course of the simulation. Frequently visited, face sharing cells were then grouped into one site. Here, the cells are shown as spheres, where cells constituting distinct lithium sites are given different colors.

pendent set of sites (B sites). Specifically, when the temperature is increased, some sites merge and some new sites become available. Further analysis showed that the B sites exhibit distinctly smaller occupation numbers n_s and effective radii $R_s = (3V/4\pi)^{1/3}$ than the A sites so that they contribute to the drops observed for these quantities in Fig. 1(a). The B sites are also separated by unusually small center-of mass distances r_{cm} from at least one other site. To further study the nature of the lithium sites, we calculate the occupation number of site i under the condition that site j is occupied, n_{ij}, and normalize it by the regular occupation number of site i, n_i. Then, a ratio $n_{ij}/n_i \approx 1$ is observed for all A sites, indicating an independent occupation of these sites, while values $n_{ij}/n_i \ll 1$ are found for the B sites and, hence, their population is suppressed by the population of other sites. Finally, from inspection of the probabilities p_{ij} that a jump from site i leads to a site j, it becomes clear that many B sites are predominantly exited towards a particular other site, as is expected for satellite sites.

These findings show that some of the lithium sites resulting from our preliminary analysis are indeed satellite or transition sites and, hence, their explicit consideration is not necessary.[51] To determine the "relevant" lithium sites, we start from the set identified at $T = 390\,\mathrm{K}$ and combine any sites i and j if at least three of the following four criteria are fulfilled: (i) the sites merge at higher T, (ii) the sites are separated by a center-of mass distance $r_{cm} < 2.0\,\text{Å}$, which is smaller than the minimum Li-Li interatomic distance, i.e., $g_{LiLi}(r < 2.0\,\text{Å}) = 0$, (iii) a ratio $n_{ij}/n_i < 0.3$ indicates that the sites are not independently occupied and (iv) a value $\max[p_{ij}, p_{ji}] > 0.5$ shows that jumps from one of the sites predominantly lead to the other. As a result, we find that all B sites identified at $T = 390\,\mathrm{K}$ are associated with an A site, leading to a number of 166 independent lithium sites. This final set of lithium sites is shown in Fig. 2. We see that the sites are compact, mostly globular objects, which are well separated from each other. All further analysis is based on these sites. However, we determined that our conclusions are not affected when the following analysis is performed on the preliminary sets of sites. Moreover, we ensured that the first and the second half of our production runs, respectively, yield nearly identical sets of sites.

IV. RESULTS

A. Properties of the lithium sites

Analyzing the ionic trajectories, we find that, for all studied T, more than 96% of the lithium positions lie within the volume constituted by the 166 lithium sites, i.e., within a volume fraction of only 1%. These percentages show that our approach allows us a complete identification of the lithium sites. In addition, they imply that the positions of the lithium sites are temperature and time independent, which in turn suggests that structural relaxation of the phosphate matrix plays no substantial role on the time scale of our simulation. Consistently, we observe that the lithium sites exhibit temperature independent properties, i.e., sites with relatively long (short) mean residence times τ_s, high (low) occupation numbers n_s, etc. at a given T show the same features at the other T studied here.

To investigate the dynamics of the phosphate matrix in more detail, we calculate the mean square displacements of the oxygen and phosphorus atoms, $r^2_{\mathrm{O}}(t)$ and $r^2_{\mathrm{P}}(t)$, respectively. Values $r^2_{\mathrm{O,P}}(10\,\mathrm{ns}) < 0.6\,\text{Å}^2$ indicate that substantial structural relaxation of the phosphate matrix is absent at the studied T. To obtain further insights, we determine the number of phosphorus atoms in the first neighborshells of the oxygen atoms, i.e., we identify bridging oxygens (BO) and nonbridging oxygens (NBO). For all T, we find that more than 98% of the oxygen atoms have the same number of phosphorus neighbors at the beginning and at the end of our 20 ns-time window and, hence, each oxygen atom has a preferred phosphorus coordination. However, there are temporary matrix fluctuations. For example, when we analyze configurations at 1000 equidistant times during $t_{sim} = 20\,\mathrm{ns}$, we observe that the fraction of oxygen atoms that *never* changes the number of phosphorus neighbors is reduced to 75% for $T = 520\,\mathrm{K}$.

Motivated by the finding that the spatial distribution of NBO is basically static on the time scale of our sim-

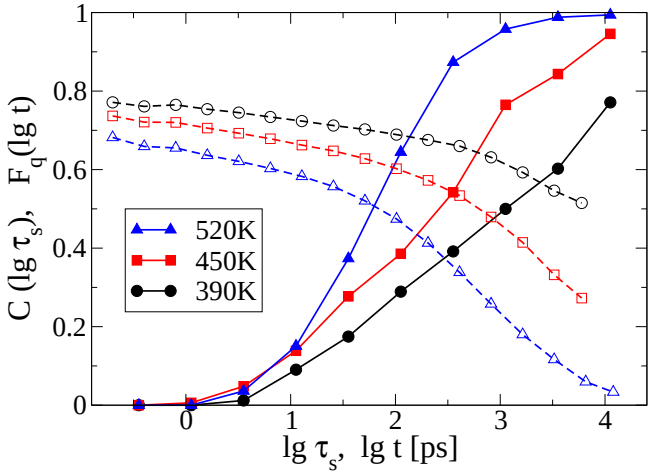

FIG. 3: Solid symbols: Cumulative distribution $C(\lg \tau_s)$ characterizing the mean residence times of the lithium ions at the sites. Open symbols: Incoherent intermediate scattering function of the lithium ions, $F_q(\lg t)$, for $q = 2\pi/r_{LiLi} = 2.3\,\text{Å}^{-1}$.

ulation, we next study the relative positions of lithium sites and NBO. For this purpose, we identify the oxygen atoms in the first neighborshells of lithium ions residing at a site and determine the fraction of NBO among this subset of oxygens. A statistical analysis shows that the fraction amounts to more than 96% at the studied T and, hence, a lithium ion at a site is predominantly surrounded by NBO. In other words, the lithium sites are located in regions with high local concentrations of NBO. For comparison, as expected for the meta-phosphate composition, the fraction of NBO among all oxygens in the system amounts to 2/3.

Figure 1(b) displays the effective radii R_s of the 166 lithium sites together with their occupation numbers n_s at $T = 390\,\text{K}$. We see that most sites are characterized by radii $R_s \approx 0.5$Å, indicating that the sites are compact objects of similar size, consistent with the appearance of Fig. 2. Further, we observe that the vast majority of the sites exhibits occupation numbers $n_s \lesssim 1$, i.e., they can accommodate only one ion at a time, so that the total number of available sites, N_s, is approximately given by the number of identified sites. Hence, the number of sites, $N_s \approx 166$, is only slightly bigger than the number of ions, $N_{\text{Li}} = 160$. Consistently, Heuer and coworkers[51] reported $N_s \approx N_{\text{Li}}$ for Li_2SiO_3 glass and proposed to describe lithium dynamics in terms of mobile vacancies. Moreover, Dyre[59] argued based on general reasoning that a minimum number of alkali sites is formed during the freezing of the network at T_g due to energetic reasons.

Next, we characterize the mean residence times τ_s at the lithium sites by the cumulative distribution $C(\lg \tau_s)$. The latter is related with the distribution of mean residence times, $G(\lg \tau_s)$, by

$$C(\lg \tau_s) = \int_{-\infty}^{\lg \tau_s} G(\lg \tau_s')\, d \lg \tau_s'$$

so that the cumulative distribution measures the fraction of sites with residence times smaller than τ_s. In Fig. 3, we see that $C(\lg \tau_s)$ shifts to longer times with decreasing T, reflecting the slowing down of lithium jump dynamics. Furthermore, the rise of $C(\lg \tau_s)$ is more gradual at lower T and, hence, the distribution $G(\lg \tau_s)$ broadens upon cooling. In particular, the increase of $C(\lg \tau_s)$ extends over more than four orders of magnitude at $T = 390\,\text{K}$, indicating that the sites feature very diverse lithium jump dynamics, i.e., pronounced dynamic heterogeneities exist. In addition, it becomes clear from Fig. 3 that about 20% of the lithium ions uninterruptedly reside at the same site during our production run for $T = 390\,\text{K}$, and, thus, the mean residence time of these sites cannot be determined. In the following analysis, we use $\tau_s = 40\,\text{ns} \equiv 2t_{sim}$, which may somewhat affect the results for $T = 390\,\text{K}$.

For comparison, we consider the incoherent intermediate scattering function of the lithium ions,

$$F_q(t) = \langle \cos\{ \vec{q}\,[\vec{r}(t_0+t) - \vec{r}(t_0)]\} \rangle.$$

Here, $\vec{r}(t)$ is the position of a lithium ion at a time t and the brackets $\langle \ldots \rangle$ denote the ensemble average. To study lithium dynamics on the length scale of the Li-Li interatomic distance, $r_{LiLi} = 2.7$Å, we use an absolute value of the wave vector $q = 2\pi/r_{LiLi}$, as was done previously.[44] In Fig. 3, we show the temperature dependence of $F_q(\lg t)$. Comparing $C(\lg \tau_s)$ and $F_q(\lg t)$ for $T = 450\,\text{K}$, we see that the latter function does not decay to zero on a time scale of 10 ns ($\lg t[\text{ps}] = 4$) and, hence, a significant fraction of lithium ions still occupies the initial site, whereas $C(\lg \tau_s[\text{ps}] = 4) \approx 1$ indicates that the residence times at nearly all sites were interrupted by jumps to other sites during this time window. In combination, these findings suggest that there is a substantial fraction of unsuccessful escape processes, i.e., the ions jump back to the initial site. Thus, the results of this section confirm our previous findings[44] that both dynamic heterogeneities and correlated back-and-forth jumps are important features of lithium jump dynamics in $LiPO_3$ glass. As will be demonstrated below, the present approach allows us to study the origin of these phenomena in detail.

B. Mechanism for the lithium jumps

To analyze the mechanism for the lithium jumps, we determine the mean jump time τ_j and the mean jump length l_j, where we define the former as the time an ion spends outside any site when it moves from one site to another and the latter as the center-of mass distance of two consecutively visited sites. At the studied T, we find mean jump times $\tau_j = 0.6 - 1.7\,\text{ps}$ that are much shorter than the mean residence times τ_s, cf. Fig. 3, confirming that jump diffusion occurs. The mean jump lengths $l_j = 3.2 - 3.7\,\text{Å}$ are only slightly bigger than the interatomic distance $r_{\text{LiLi}} = 2.7\,\text{Å}$ and, thus, the lithium ions predominantly jump to neighboring sites.

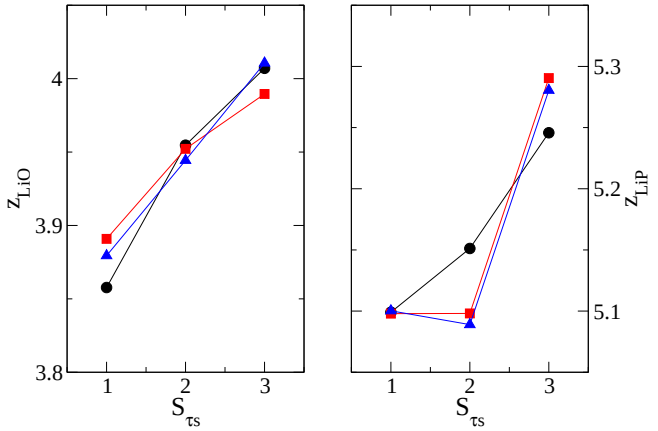

FIG. 4: Mean coordination numbers (a) z_{LiO} and (b) z_{LiP} for lithium ions residing at sites with short ($S_{\tau s}=1$), medium ($S_{\tau s}=2$) and long ($S_{\tau s}=3$) mean residence times τ_s. Each subset contains about 1/3 of all sites. For example, $S_{\tau s}=1$ consist of sites with residence times $\tau_s<\tau_1$, where $C(\lg\tau_1)=1/3$.

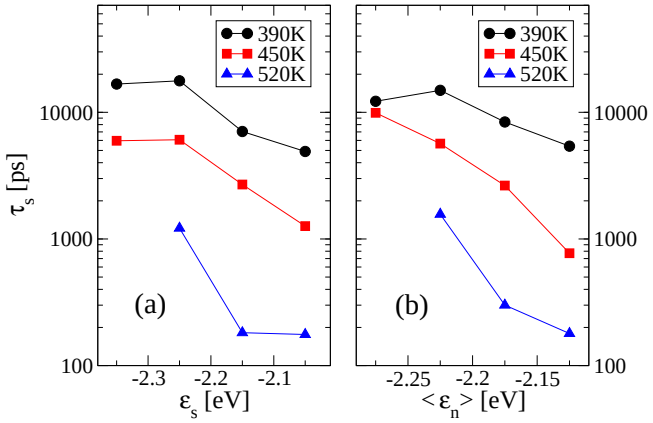

FIG. 5: Mean residence times τ_s at the lithium sites plotted as a function of (a) the site energy ε_s and (b) the average site energy of the neighboring sites, $\langle\varepsilon_n\rangle$.

When we consider the very limited number of lithium sites $N_s \approx N_{\mathrm{Li}}$, there are two possible mechanisms for the repopulation of the sites. On the one hand, one can imagine a vacancy mechanism where a site is first exited by ion A and immediately afterwards occupied by ion B. Indeed, studying examples of ionic trajectories, a vacancy-like mechanism was observed for a silicate glass.[41] On the other hand, it is possible that ion B enters an occupied site and "kicks out" ion A. Both scenarios can be distinguished when we determine the probability that a lithium jump leads to an empty site. We find that this probability is higher than 84% in the considered temperature range, indicating that a vacancy mechanism dominates the repopulation of the lithium sites.

C. Origin of the dynamic heterogeneities

The relation between the lithium jump dynamics and the local glass structure can be studied when we analyze the environments of sites with diverse mean residence times. Therefore, we now compare the mean coordination numbers of lithium ions at sites with short ($S_{\tau s}=1$), medium ($S_{\tau s}=2$) and long ($S_{\tau s}=3$) residence times τ_s. In Fig. 4, we see that, on average, lithium ions at sites with short τ_s exhibit smaller mean coordination numbers z_{LiO} and z_{LiP} than those ions at sites with long τ_s. This suggests that sites featuring slow lithium jumps are well embedded in the phosphate-glass matrix, however, the effects are weak. For the mean coordination number z_{LiLi}, we observe no significant correlation. Also, we find no systematic effects due to other quantities characterizing the local lithium environments. Hence, our results give no evidence that any particular structural property determines the lithium jump dynamics in $LiPO_3$ glass. However, the local structure determines the local energy landscape. We find that the average energy of a lithium ion at a site, or, equivalently, the site energy ε_s is relatively low for sites where the lithium ions have oxygen neighbors that contain a high fraction of NBO. In the following, we directly study the effects of the local energy landscape on lithium jump dynamics.

To determine the site energy ε_s of a given site and for a given T, we identify the lithium ion, if any, that occupies this site in a considered MD configuration at this T, calculate its potential energy using Eq. 1 and average over many configurations. Figure 5(a) shows τ_s as a function of the site energies ε_s. As may be expected, the mean residence time decreases with increasing ε_s. However, decays by factors of between five and ten are small compared to the width of $G(\lg\tau_s)$, which spans at least three orders of magnitude, see Fig. 3. For example, if a random trap model were an appropriate description, i.e., if the residence time were exclusively determined by ε_s, a decline of τ_s by a factor of ~ 2000 would be expected based on $\Delta\tau_s = \exp[\Delta\varepsilon_s/(k_B T)]$, $\Delta\varepsilon_s = 0.3\,\mathrm{eV}$ and $T = 450\,\mathrm{K}$. Thus, the jump rate at a site depends not only on ε_s, but there are additional factors. For example, the energy barriers separating the sites may show a distribution of barrier heights, as expected for the energy landscape of a disordered material.

Another important factor can be inferred from an inspection of Fig. 5(b), where the mean residence time at a site is plotted as a function of the average site energy, $\langle\varepsilon_n\rangle$, of all *neighboring* sites. Here, we define neighboring sites based on the criterion that their center-of mass distance r_{cm} be smaller than the distance corresponding to the first minimum of the Li-Li pair correlation function. Interestingly, we observe that τ_s strongly decreases with increasing $\langle\varepsilon_n\rangle$, indicating that, on average, sites surrounded by high energetic neighbors feature fast lithium dynamics. On first glance, this result is counterintuitive since one would expect that jumps to sites with comparatively high site energies are characterized by small rates and, hence, sites with high values of $\langle\varepsilon_n\rangle$ should exhibit

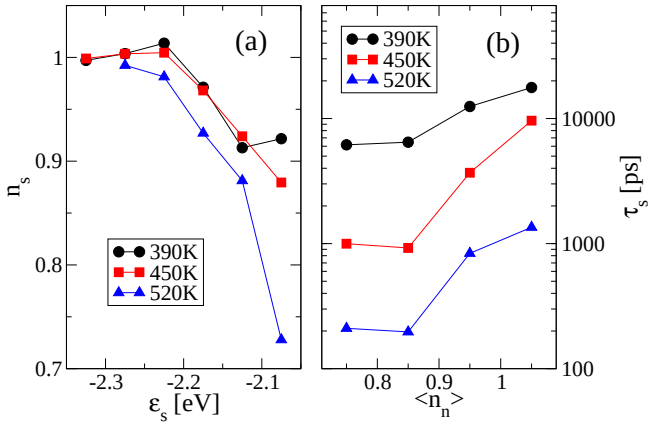

FIG. 6: (a) Mean number n_s of lithium ions at a site as a function of the site energy ε_s. (b) Mean residence time τ_s at a lithium site as a function of n_s.

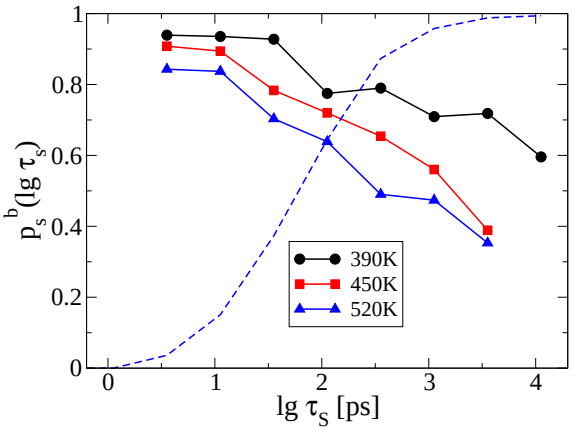

FIG. 7: Backjump probability p_s^b as a function of the logarithm of the mean residence time, $\lg \tau_s$, for various temperatures. Dashed line: Cumulative distribution of the mean residence time, $C(\lg \tau_s)$, for $T = 520\,\mathrm{K}$.

long τ_s.

However, a decrease of τ_s with $\langle \varepsilon_n \rangle$ can be understood when we consider our result that a vacancy mechanism dominates the redistribution of a small fraction of empty sites. In such scenario, the ionic jump rates are first of all limited by the availability of a vacant neighboring site. In Fig. 6(a), we see that the occupation numbers n_s are smaller for sites with high site energies ε_s, as may be expected. Thus, when the neighbors of a site A exhibit high site energies, these neighbors are often unoccupied so that ions at site A frequently have the chance for a jump. Consequently, in our case of a vacancy mechanism, it is plausible that sites characterized by high values of $\langle \varepsilon_n \rangle$ show relatively short τ_s, as is observed in Fig. 5(b). To further check our argumentation, we plot the mean residence time at a site as a function of the average occupation number, $\langle n_n \rangle$, of all neighboring sites in Fig. 6(b). We see that τ_s strongly grows with $\langle n_n \rangle$, supporting our conclusion that lithium diffusion in $LiPO_3$ glass is governed by the competition of the ions for a small fraction of vacant sites. These results clearly show that single-particle approaches do not allow a complete understanding of ion dynamics in glasses.

D. Correlated back-and-forth jumps

The results of our previous work[44] and the discussion of Fig. 3 imply that correlated back-and-forth jumps are another feature of lithium dynamics in the studied model. To investigate this effect in more detail, we calculate the backjump probability P^b of finding a lithium ion at the same site after exactly two jumps. Analyzing all jumps during our production runs, we find that the backjump probability increases from $P^b = 0.77$ at $T = 520\,\mathrm{K}$ to $P^b = 0.91$ at $T = 390\,\mathrm{K}$. For comparison, a value $P^b \approx 0.25$ would result for a random walk since, on average, each lithium site has about four neighboring sites. Thus, the observed backjump probabilities clearly indicate that correlated back-and-forth jumps are an important phenomenon in the studied temperature range.

To obtain further insights, we next determine the site-dependent backjump probability p_s^b, i.e., for each site, we calculate the probability that a jump from this site to another site is followed by a direct backjump. Motivated by results of Heuer and coworkers,[51] we then study the relation between the backjump probability p_s^b and the mean residence time τ_s. From the results in Fig. 7, it is evident that the backjump probability is higher at lower T. Furthermore, we see that p_s^b strongly decreases with increasing $\lg \tau_s$. Specifically, comparison with the cumulative distribution $C(\lg \tau_s)$ shows that about 90% of the jumps starting from sites with short $\lg \tau_s$ are followed by a direct backjump, whereas backjumps occur with nearly statistical probability, $p_s^b \approx 0.25$, after the escape from sites with long τ_s. Reinspecting also $F_q(\lg t)$ in Fig. 3, these findings show that lithium hopping on the time scale of the lithium relaxation resembles a random walk, whereas ions that exit their sites at much earlier times very often return to these sites, i.e., such jumps are unsuccessful. A similar behavior was observed for lithium silicate glasses by Heuer and coworkers.[51]

Finally, we analyze the relation between the backjump probability and the local energy landscape. In Fig. 8(a), we see that, on average, sites with high site energies ε_s show somewhat higher values of p_s^b. Figure 8(b) displays p_s^b as a function of the average energy, $\langle \varepsilon_n \rangle$, of the neighboring sites. Obviously, the backjump probability hardly depends on $\langle \varepsilon_n \rangle$. When we assume single-particle motion in an energy landscape, these results are difficult to understand. In such approach, jumps to sites with lower site energies are favored and, hence, the backjump probability should be high for sites characterized by small values of ε_s and high values of $\langle \varepsilon_n \rangle$, at variance with our observations. Hence, our findings for the back-and-forth dynamics again suggest that multiparticle interactions are important for the lithium jumps in $LiPO_3$ glass. We

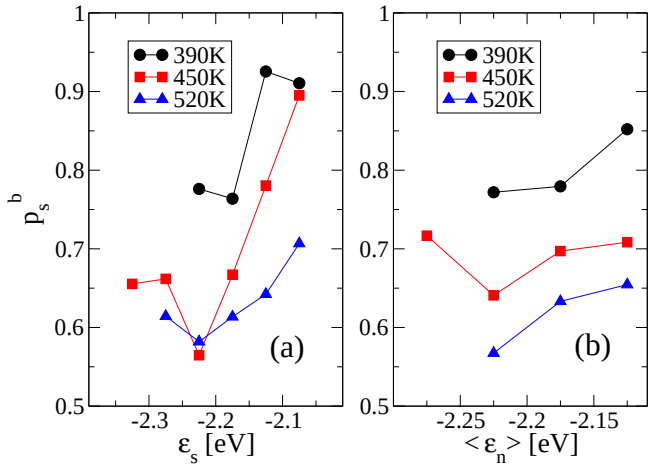

FIG. 8: Backjump probability p_s^b as a function of (a) the site energy ε_s and (b) the average site energy of the neighboring sites, $\langle\varepsilon_n\rangle$.

add that we find no evidence for a systematic dependence of p_s^b on properties of the local glass structure such as the mean coordination numbers z_{LiO}, z_{LiP} and z_{LiLi}.

V. DISCUSSION AND SUMMARY

We performed MD simulations to investigate lithium dynamics in $LiPO_3$ glass at temperatures where the phosphate matrix is basically rigid on the time scale of our simulation. We observed that lithium ionic migration in this glassy matrix results from jumps between well defined sites. Making use of a straightforward algorithm,[51] the lithium sites were completely identified from the ionic trajectories. The results show that the sites are typically compact objects of similar size and globular shape. Moreover, the number of lithium sites hardly outnumbers the number of lithium ions, as was observed for lithium silicate glasses.[51] Characterizing the structural and dynamical features of the sites, we found that these properties are unmodified on the time scale of the lithium ionic relaxation. This allowed us to systematically study the relationship between structure and dynamics.

Analyzing the phosphate dynamics in detail, we found that the glassy matrix, apart from temporary fluctuations, is static on the 20 ns-time scale of our simulation. In particular, there is a basically time independent spatial distribution of NBO. While one may speculate whether the temporary matrix fluctuations assist the lithium jumps, as was observed for other ionic glasses,[60,61] the present results are at variance with a substantial structural relaxation of the glassy matrix, e.g., a redistribution of NBO, as was proposed in previous work.[16,18] Instead, the properties of the lithium sites are determined by the configuration frozen in at the glass transition. In particular, we observed that the lithium sites are located in regions with high local concentrations of NBO so that most lithium ions at a site are exclusively surrounded by this oxygen species. Though we do not expect that our findings are unique to $LiPO_3$ glass, we cannot exclude that the scenario changes for small alkali concentrations, where NBO may be formed along the alkali trajectories.[62]

Mapping the lithium trajectories onto sequences of jumps between the identified sites, we analyzed the mechanism for the ionic diffusion. The mean jump times and the mean jump lengths indicated that lithium migration results from hopping between neighboring sites. A statistical analysis of the repopulation of the lithium sites showed that the sites are usually first vacated by one ion and shortly afterwards entered by another ion, implying that lithium hopping is governed by a vacancy mechanism. Such mechanism is reasonable in a situation where the number of alkali sites is only slightly bigger than the the number of alkali ions, as is the case both in lithium silicate glasses[51] and in our model of a lithium phosphate glass. For silicate glasses, a vacancy-like mechanism was also observed when inspecting examples of ionic trajectories.[41]

To characterize the average dynamical behavior of a lithium ion at a particular site, we determined the mean residence times τ_s at the sites. We found that the sites feature a broad distribution $G(\lg\tau_s)$, indicating the existence of pronounced dynamic heterogeneities. $G(\lg\tau_s)$ broadens upon cooling so that the distribution extends over more than four orders of magnitude at the lowest T studied. Consistently, we observed in our previous MD study of $LiPO_3$ glass[44] that dynamic heterogeneities increasingly contribute to the nonexponential lithium relaxation upon cooling. All these simulation results are in agreement with findings from multidimensional NMR experiments on silver phosphate glasses,[30,31] which show that a very broad distribution of jump rates governs silver dynamics at low T, where the silver relaxation occurs on the time scale of ms − s.

The present approach provides direct access to the origin of the dynamic heterogeneities. We observed that, on average, lithium ions at sites with long τ_s show somewhat higher coordination numbers z_{LiO} and z_{LiP}, suggesting that these sites are located in a matrix-rich environment. However, the direct effects of the local glass structure on the lithium jump dynamics are weak. On the other hand, the local structure determines the local energy landscape, which in turn strongly affects the residence times. Specifically, as may be expected, we found that τ_s decreases with the site energy ε_s. More interestingly, τ_s also declines when the average site energy $\langle\varepsilon_n\rangle$ of the neighboring sites increases. Such behavior is difficult to capture within single-particle approaches on ion transport in glasses, including percolation approaches. However, it can be understood when we consider our results that there is a small fraction of empty sites that are redistributed in a vacancy mechanism. In such scenario, the jump rates are limited by the restricted access to a vacant site. Due to a correlation between the energies ε_s

and the occupation numbers n_s of the sites, the probability of finding a vacant neighboring site is high when the latter exhibit high site energies and, consequently, τ_s is expected to decrease with $\langle\varepsilon_n\rangle$, in agreement with our observation. We conclude that the pronounced dynamic heterogeneities in $LiPO_3$ glass result from both a disordered energy landscape and a distribution of probabilities of having access to a vacant neighboring site.

We also calculated the site-dependent backjump probability p_s^b that a jump from a particular site to another site is followed by a direct backjump. Such analysis allowed us to quantify the importance of correlated back-and-forth jumps. We found that p_s^b strongly depends on the mean residence time τ_s, i.e., on the dynamical state of an ion. High values of p_s^b for sites with short τ_s indicate that correlated back-and-forth jumps are a relevant feature of lithium dynamics at the studied T. Specifically, backjump probabilities $p_s^b \approx 0.9$ that increase upon cooling show that only $\sim 10\%$ of the jumps starting from sites with short τ_s are successful and, hence, ion transport is substantially slowed down due to back-and-forth jumps, in particular at low T. In contrast, sites characterized by long τ_s show backjump probabilities that are close to the value expected for a random jump. These results for $LiPO_3$ glass are in agreement with findings for lithium silicate glasses by Heuer and coworkers,[51] implying that there is a similar mechanism for lithium jump dynamics in different types of glasses. However, correlated back-and-forth jumps were not observed in a computational study of ion dynamics at comparatively high T.[47] This apparent discrepancy may be reconciled by our result that the importance of this phenomenon decreases with increasing T.

Our results may also help to unravel two puzzling effects related to ion dynamics. As aforementioned, applications of different experimental techniques lead to different conclusions about the relevance of correlated back-and-forth jumps. These discrepancies may be explained by the strong dependence of the backjump probability on the dynamical state of an ion. Similar to Heuer and coworkers,[51] we argue that the observed correlated back-and-forth jumps of the fast ions dominate the dispersive regime of the electric conductivity $\sigma(\nu)$.[6,24,25,26,27] An additional contribution to the dispersion may result from fast forward-backward motions on length scales shorter than the Li-Li interatomic distance, e.g., jumps between sites and their satellites, which are not considered in the present analysis. In contrast, studying the dynamical behavior of subensembles of slow ions in multidimensional NMR experiments,[31,32] no evidence for correlated back-and-forth jumps was found. Consistently, we observed that lithium dynamics on the time scale of the lithium relaxation resembles a random walk.

The second puzzling effect concerns the approximate time-temperature superposition observed for the incoherent intermediate scattering function $F_q(t)$ in simulation studies.[42,44] This behavior is surprising since both dynamic heterogeneities[43,44] and back-and-forth jumps become more important with decreasing T, see Figs. 3 and 7, and, hence, one might be tempted to conclude that the nonexponentiality of $F_q(t)$ should increase upon cooling. However, such simple argumentation is only possible when the backjump probability is independent of the dynamical state. Here, the back-and-forth jumps of the fast ions shift the time t_0 when $F_q(t)$ starts to decay to longer times, while the time t_1 when the decay of $F_q(t)$ is complete is not affected due to back-and-forth dynamics because no enhanced back-jump probability exists for the slow ions. This means that, in our case, back-and-forth jumps *reduce* the time interval $t_1 - t_0$, i.e., the nonexponentiality of $F_q(t)$. Hence, when T is lowered, there are two competing effects. While the increasing heterogeneity of dynamics leads to a stronger nonexponentiality, the growing backjump probability of the fast ions delays the onset of the decay, t_0, further and further and, hence, reduces the nonexponentiality. Thus, both effects may compensate each other, resulting in a nearly temperature independent nonexponentiality of $F_q(t)$.

In summary, we found that, in a model of $LiPO_3$ glass, the disordered energy landscape provided by the phosphate-glass matrix plays a major role for the lithium jump dynamics. For a complete understanding of the jump-diffusion mechanism, single-particle approaches are not sufficient, but rather it is importont to consider the competition of the lithium ions for a small fraction of vacant sites at every instant. As a consequence, the dynamical behavior is highly complex. In particular, pronounced dynamic heterogeneities exist and the backjump probability depends on the dynamical state of an ion.

Acknowledgments

I thank S. C. Glotzer for a generous grant of computer time and A. Heuer, H. Lammert and J. Reinisch for many stimulating discussions. Funding of the Deutsche Forschungsgemeinschaft through the Emmy Noether-Programm is gratefully acknowledged.

* Electronic address: mivogel@uni-muenster.de
† Institut für Physikalische Chemie, Westfälische Wilhelms-Universität Münster, Corensstr. 30, 48149 Münster, Germany

[1] A. Bunde, M. D. Ingram and P. Maass, J. Non-Cryst. Solids 172-174, 1222 (1994)
[2] K. L. Ngai, J. Non-Cryst. Solids 203, 232 (1996)
[3] A. Bunde, K. Funke and M. D. Ingram, Solid State Ionics 105, 1 (1998)
[4] K. Funke, Prog. Solid State Chem. 22, 111 (1993)

[5] S. R. Elliott, Solid State Ionics 70/71, 27 (1994)
[6] K. Funke, B. Roling and M. Lange, Solid State Ionics 105, 195 (1998)
[7] J. M. Stevels, in *Handbuch der Physik*, Vol. 20, edited by S. Flügge, Springer Verlag, Berlin (1957)
[8] M. D. Ingram, Philos. Mag. B 60, 729 (1989)
[9] J. C. Dyre and T. B. Schrøder, Rev. Mod. Phys. 72, 873 (2000)
[10] I. Svare, F. Borsa, D. R. Torgeson and S. W. Martin, Phys. Rev. B 48, 9336 (1993)
[11] S. Sen, A. M. George and J. F. Stebbins J. Non-Cryst. Solids 197, 53 (1996)
[12] S. D. Baranovskii and H. Cordes, J. Chem. Phys. 111, 7546 (1999)
[13] P. Maass, J. Petersen, A. Bunde, W. Dieterich and H. E. Roman, Phys. Rev. Lett. 66, 52 (1991)
[14] P. Maass, M. Meyer, A. Bunde and W. Dieterich, Phys. Rev. Lett. 77, 1528 (1996)
[15] D. Knödler, P. Penzig and W. Dieterich, Solid State Ionics 86-88, 29 (1996)
[16] G. N. Greaves and K. L. Ngai, Phys. Rev. B 52, 6358 (1995)
[17] G. N. Greaves, J. Non-Cryst. Solids 71, 203 (1985)
[18] P. Maass, A. Bunde and M. D. Ingram, Phys. Rev. Lett. 68, 3064 (1992)
[19] C. T. Moynihan, L. P. Boesch and N. L. Laberge, Phys. Chem. Glasses 14, 122 (1973)
[20] C. Liu and C. A. Angell, J. Non-Cryst. Solids 83, 162 (1986)
[21] P. F. Green, D. L. Sidebottom and R. K. Brow, J. Non-Cryst. Solids 172-174, 1353 (1994)
[22] P. F. Green, E. F. Brown and R. K. Brow, J. Non-Cryst. Solids 255, 87 (1999)
[23] R. Böhmer, R. V. Chamberlin, G. Diezemann, B. Geil, A. Heuer, G. Hinze, S. C. Kuebler, R. Richert, B. Schiener, H. Sillescu, H. W. Spiess, U. Tracht and M. Wilhelm, J. Non-Cryst. Solids 235-237, 1 (1998)
[24] A. K. Jonscher, Nature 267, 673 (1977)
[25] S. W. Martin and C. A. Angell, J. Non-Cryst. Solids 83, 185 (1986)
[26] K. Funke and C. Cramer, Curr. Opin. Solid State Mater. Sci. 2, 483 (1997)
[27] B. Roling, A. Happe, K. Funke and M. D. Ingram, Phys. Rev. Lett. 78, 2160 (1997)
[28] R. Böhmer, T. Jörg, F. Qi and A. Titze, Chem. Phys. Lett. 316, 419 (2000)
[29] F. Qi, T. Jörg and R. Böhmer, Solid State Nucl. Magn. Reson. 22, 484 (2002)
[30] M. Vogel, C. Brinkmann, H. Eckert and A. Heuer, J. Non-Cryst. Solids 307-310, 971 (2002)
[31] M. Vogel, C. Brinkmann, H. Eckert and A. Heuer, Phys. Chem. Chem. Phys. 4, 3237 (2002)
[32] M. Vogel, C. Brinkmann, H. Eckert and A. Heuer, Phys. Rev. B (in press)
[33] W. Smith, G. N. Greaves and M. J. Gillan, J. Chem. Phys. 103, 3091 (1995)
[34] S. Balasubramanian and K. J. Rao, J. Non-Cryst. Solids 181, 157 (1995)
[35] A. Karthikeyan and K. J. Rao, J. Phys. Chem. B 101, 3105 (1997)
[36] D. Timpel and K. Scheerschmidt, J. Non-Cryst. Solids 232-234, 245 (1998)
[37] J. Kieffer, J. Non-Cryst. Solids 255, 56 (1999)
[38] B. Park and A. N. Cormack, J. Non-Cryst. Solids 255, 112 (1999)
[39] J. Horbach, W. Kob and K. Binder, Chem. Geology 174, 87 (2001)
[40] J. Habasaki and Y. Hiwatari, Phys. Rev. E 65, 021604 (2002)
[41] A. N. Cormack, J. Du and T. R. Zeitler, Phys. Chem. Chem. Phys. 4, 3193 (2002)
[42] A. Heuer, M. Kunow, M. Vogel and R. D. Banhatti, Phys. Chem. Chem. Phys. 4, 3185 (2002)
[43] A. Heuer, M. Kunow, M. Vogel and R. D. Banhatti, Phys. Rev. B. 66, 224201 (2002)
[44] M. Vogel, Phys. Rev. B 68, 184301 (2003)
[45] P. Jund, W. Kob and R. Jullien, Phys. Rev. B 64, 134303 (2001)
[46] E. Sunyer, P. Jund and R. Jullien, Phys. Rev. B 65, 214203 (2002)
[47] E. Sunyer, P. Jund, W. Kob and R. Jullien, J. Non-Cryst. Solids, 307-310, 939 (2002)
[48] J. Horbach, W. Kob and K. Binder, Phys. Rev. Lett. 88, 125502 (2002)
[49] E. Sunyer, P. Jund and R. Jullien, J. Phys.: Condens. Matt. 15, S1659 (2003)
[50] B. Vessal, G. N. Greaves, P. T. Martin, A. V. Chadwick, R. Mole and S. Houde-Walter, Nature (London) 356, 504 (1992)
[51] H. Lammert, M. Kunow and A. Heuer, Phys. Rev. Lett. 90, 215901 (2003)
[52] A. Karthikeyan, P. Vinatier, A. Levasseur and K. J. Rao, J. Phys. Chem. B 103, 6185 (1999)
[53] J.-J. Liang, R. T. Cygan and T. M. Alam, J. Non-Cryst. Solids 263-264, 167 (2000)
[54] U. Hoppe, G. Walter, R. Kranold and D. Stachel, J. Non-Cryst. Solids 263-264, 29 (2000)
[55] R. K. Brow, J. Non-Cryst. Solids 263-264, 1 (2000)
[56] L. van Wüllen, H. Eckert and G. Schwering, Chem. Mater. 12, 1840 (2000)
[57] K. Muruganandam, M. Seshasayee and S. Patanaik, Solid State Ionics 89, 313 (1996)
[58] S. English and W. E. S. Turner, J. Am. Ceram. Soc. 13, 182 (1930)
[59] J. Dyre, J. Non-Cryst. Solids 307, 939 (2002)
[60] E. Sunyer, P. Jund and R. Jullien, J. Phys.: Condens. Matt. 15, L431 (2003)
[61] C. A. Angell, L. Boehm, P. A. Cheeseman and S. Tamaddon, Solid State Ionics 5, 659 (1981)
[62] J. Oviedo and J. F. Sanz, Phys. Rev. B 58, 9047 (1998)